Signaling events at TMEM doorways provide potential targets for inhibiting breast cancer dissemination

Chinmay R. Surve[1,5‡], Camille L. Duran[1,2,3,4,5,‡,*], Xianjun Ye[1,2,3,4,5], Xiaoming Chen[2,3], Yu Lin[2,3], Allison S. Harney[1,5], Yarong Wang[1], Ved P. Sharma[2,5], E. Richard Stanley[6], John C. McAuliffe[1,2,3,4,7], David Entenberg[1,2,3,4,5], Maja H. Oktay[1,2,3,4,7,*] and John S. Condeelis[1,3,4,5,7,*]

[1]Integrated Imaging Program for Cancer Research, [2]Department of Pathology, [3]Montefiore Einstein Comprehensive Cancer Center, [4]Cancer Dormancy and Tumor Microenvironment Institute, [5]Gruss-Lipper Biophotonics Center, [6]Department of Cell Biology, [7]Department of Surgery, Albert Einstein College of Medicine, Bronx, New York. [‡] These authors contributed equally to this work.

***Address for Correspondence:**

Camille L. Duran
Maja H. Oktay
John S. Condeelis
Albert Einstein College of Medicine
Department of Cell Biology
Department of Pathology
1300 Morris Park Ave
Bronx, NY 10461
Email:
camille.duran@einsteinmed.edu
moktay@montiefore.org
john.condeelis@einsteinmed.edu

Abstract:

Tumor cell intravasation is essential for metastatic dissemination, but its exact mechanism is incompletely understood. We have previously shown that in breast cancer, the direct and stable association of a tumor cell expressing Mena, a Tie2^{hi}/Vegf^{hi} macrophage, and a vascular endothelial cell, creates an intravasation portal, called a “tumor microenvironment of metastasis” (TMEM) doorway, for tumor cell intravasation, leading to dissemination to distant sites. The density of TMEM doorways, also called TMEM doorway score, is a clinically validated prognostic marker of distant metastasis in breast cancer patients. Although we know that tumor cells utilize TMEM doorway-associated transient vascular openings to intravasate, the precise signaling mechanisms involved in TMEM doorway function are only partially understood.

Using two mouse models of breast cancer and an *in vitro* assay of intravasation, we report that CSF-1 secreted by the TMEM doorway tumor cell stimulates local secretion of VEGF-A from the Tie2^{hi} TMEM doorway macrophage, leading to the dissociation of endothelial junctions between TMEM doorway associated endothelial cells, supporting tumor cell intravasation. Acute blockage of CSF-1R signaling decreases macrophage VEGF secretion as well as TMEM doorway-associated vascular opening, tumor cell trans-endothelial migration, and dissemination. These new insights into signaling events regulating TMEM doorway function should be explored further as treatment strategies for metastatic disease.

Introduction:

Metastasis is a complex, multi-step and multi-directional process that begins with the dissemination of tumor cells from the primary tumor to distant sites and escalates by further re-dissemination of cancer cells from metastatic foci(1-4). The re-dissemination process leads to an exponential increase in tumor burden and, eventually, patient demise. Tumor cell intravasation into the vasculature creates circulating tumor cells (CTCs) and is an essential step in the metastatic cascade, but its exact mechanism is not completely understood. A large body of evidence indicates that tumor cell dissemination, including tumor cell intravasation, is orchestrated by the interaction of tumor cells with the tumor microenvironment (5, 6). In particular, tumor-associated macrophages interact with tumor cells and promote directed cell migration (streaming) towards blood vessels (7-9). In addition, macrophages form a multi-cellular complex with endothelial and tumor cells on the surface of blood vessels to mediate transient vascular opening and tumor cell intravasation. These cell complexes are called TMEM (Tumor MicroEnvironment of Metastasis) doorways (10, 11). Each TMEM doorway is composed of one tumor cell expressing Mena, one $Tie2^{hi}/Vegf^{hi}$ macrophage, and a vascular endothelial cell, all in direct and stable physical contact (10, 12, 13).

TMEM doorway-associated vascular opening (TAVO) was first discovered using high-resolution intravital imaging as localized and transient bursts of intravascular contrast agents into the extravascular space that could be accompanied by concurrent intravasation of cancer cells (10). Further analyses revealed in mouse models of breast cancer, TAVO, and its associated cancer cell intravasation, occurs exclusively at TMEM doorways (10). Importantly, TMEM doorway score in primary breast tumors has been clinically validated as a prognostic marker of distant metastatic recurrence in breast cancer patients with estrogen receptor positive HER2 negative (ER+/HER2-) disease, independent of other clinical prognostics (12-14). Additionally, when comparing residual ER+/HER2- tumors from breast cancer patients after completion of pre-operative chemotherapy, Black patients were found to have a higher TMEM doorway score than white patients (15). These findings potentially provide an explanation for the persistent racial disparities in ER+/HER2- breast cancer outcomes that are not fully explained by disparities in social determinants of health, including access to care or treatment (12, 15-17). TMEM doorway score has also been found to increase during neo-adjuvant chemotherapy, suggesting that TMEM doorway score, as measured using TMEM doorway activity MRI (17), may be a useful companion diagnostic for the prediction of benefit from certain types of treatment. Given that Black compared to white patients have a higher TMEM doorway density in their residual disease after

chemotherapy, using TMEM doorway activity MRI may potentially help diminish racial disparity in breast cancer outcome (18, 19).

In humans and mice, TMEM doorways are found in pre-invasive and invasive ductal breast carcinoma, as well as in metastatic foci in lymph nodes and lungs (18-24). This suggests that the TMEM doorway-mediated mechanism of cancer cell dissemination occurs not only at the primary tumor site, but also at metastatic sites, and may contribute to the multi-directional cancer spread that perpetuates metastatic dissemination even after removal of the primary tumor (1-4, 18). Thus, understanding the molecular mechanisms of TMEM doorway function may help develop therapeutic targets to slow distant metastases and improve patient survival.

Inhibiting TMEM doorway associated vascular opening (TAVO) prevents the formation of CTCs and metastases (10). Although we know that TMEM doorways induce localized vascular opening through the secretion of vascular endothelial growth factor-A (VEGF-A) from the TMEM doorway macrophage (10), the precise signaling mechanisms involved in TMEM-doorway function during intravasation have not been elucidated. The work described here provides a greater understanding of the signaling events that regulate these dynamic, multi-cellular interactions. In particular, we report the identification of the signaling events involved in TAVO and TMEM doorway-mediated intravasation, which can serve as potential new prognostic markers and therapeutic targets for suppressing CTC dissemination and breast cancer metastasis.

Results:

CSF-1 levels are elevated in tumor cells at active TMEM doorways

Macrophage-secreted VEGF-A is critical for regulation of TMEM doorway activity (10). VEGF-A secretion from macrophages is regulated by CSF-1, also known as M-CSF (25, 26). Since tumor cells are known to secrete CSF-1 (27-29), we investigated if TMEM doorway tumor cells express CSF-1 and if this expression is associated with TMEM doorway vascular opening (10). We first determined whether CSF-1 levels are increased in TMEM doorway tumor cells at active TMEM doorways by multiplex staining of breast tumor tissue sections obtained from the *polyoma* middle T antigen (PyMT) mice injected *i.v.* with high molecular weight dextran (155 kDa, green) 1 hour before sacrifice. In these samples, if there has been a TMEM doorway associated vascular opening (TAVO) (which would indicate an active TMEM doorway), the *i.v.* injected dextran would extravasate into the intersitium and be detectable extravascularly in the tissue near a TMEM doorway **(Figure 1A)**. We used a modified approach of our previously published protocol

for detection of active TMEM doorways (30). We stained two sequential tumor sections – one using IHC for TMEM doorways **(Figure 1B**, Iba1, endomucin, Mena**)** and the other using IF for CSF-1, dextran, and endothelial cells (endomucin) **(Figure 1C)** and aligned the images of stained sections to the single cell level. We then identified which TMEM doorways were active by examining for the presence of high molecular weight dextran (155 kDa, green) in the extravascular space near the TMEM doorway, as described previously (10, 31). We then visualized and quantified the expression of CSF-1 (red) in TMEM doorway tumor cells of both active and inactive doorways **(Figure 1C)**. We observed that the fluorescence intensity of intracellular CSF-1 in TMEM doorway tumor cells was higher in active TMEM doorways **(Figure 1C, lower panel)** compared to inactive TMEM doorways **(Figure 1C, upper panel)**. This is quantified in **Figure 1D**. These results indicate that TMEM doorway tumor cells may play a significant role in regulating TMEM doorway function and activity by providing CSF1.

Tumor cells stimulate macrophage VEGF-A secretion without affecting its expression

Since CSF-1 is upregulated in the tumor cell at active TMEM doorways, and secretion of VEGF-A is known to be regulated by CSF-1 in other cell types (25, 26), we investigated the signaling interplay between the tumor cell and macrophage at the TMEM doorway. Using an ELISA, we confirmed that exogenous recombinant CSF-1 can stimulate macrophages to secrete VEGF-A **(Figure 2A)** and that tumor cells secrete CSF-1 **(Figure 2B)**. To examine the role of tumor cell secreted CSF-1 in regulating macrophage VEGF-A secretion, we first determined if TMEM doorway macrophages, characterized by expression of expression of CD68 or CD206/MRC1, express the CSF-1 receptor (CSF-1R) using immunofluorescence staining of PyMT tumors for macrophages CSF-1R, and endothelial cells (CD31) as described previously (10, 32). We confirmed that TMEM doorway macrophages do indeed express CSF-1R **(Figure 2C, D)**.

To determine if tumor cells can stimulate macrophage VEGF-A secretion, we used a human tumor cell - mouse macrophage co-culture system and quantified the amount of secreted VEGF-A by ELISA using an antibody that can only recognize mouse-derived VEGF-A, secreted by the macrophages. Co-culture of human MDA-MB-231 tumor cells with mouse BAC1.2F5 macrophages **(Figure 3A)** or culture of BAC1.2F5 macrophages with conditioned media obtained from MDA-MB-231 tumor cells **(Figure 3B)**, resulted in increased secretion of VEGF-A by the mouse-derived macrophages.

To ascertain the role of tumor cell secreted CSF-1 in stimulating macrophage VEGF-A secretion, we used the same co-culture system of MDA-MB-231 tumor cells and BAC1.2F5

macrophages as above. We inhibited CSF-1R signaling in macrophages with either a CSF-1R neutralizing antibody (CSF-1R Ab), or an inhibitor which prevents downstream signaling of the CSF-1R (CSF-1R inhibitor (GW2580)). We found that either method reduced macrophage VEGF-A secretion **(Figure 3A)**. Likewise, inhibition of CSF-1R in macrophages cultured with conditioned media obtained from the tumor cells led to a reduction in the amount of secreted VEGF-A **(Figure 3B)**. Similar results were obtained using mouse bone marrow derived primary macrophages (BMMs) **(Supplementary Figure 1A)**. Co-culturing a different breast cancer cell line, 4T1 tumor cells, which also secrete CSF-1 **(Supplementary Figure 1B)**, with BAC1.2F5 macrophages also caused an increase in VEGF-A secretion by macrophages **(Supplementary Figure 1C).** In these additional models, the increase in macrophage secretion of VEGF-A in response to tumor cell CSF-1 was again suppressed through addition of CSF-1R inhibitors or blocking antibodies **(Supplemental Figure 1A, 1C)**. Next, we used immortalized BMMs which either express (ctrl) or lack the expression of CSF-1R (C*sf1r-/-)* (33) to determine the role of macrophage CSF-1R in regulating VEGF-A secretion. Compared to the BMMs expressing CSF-1R (ctrl), which secreted VEGF-A in both the co-culture system and when cultured in tumor cell conditioned media **(Figure 3C, D)**, BMMs lacking CSF-1R (C*sf1r-/-)* did not significantly secrete VEGF-A in either a co-culture system with MDA-MB-231 tumor cells or conditioned media derived from the tumor cells **(Figure 3C, D)**.

We next evaluated if co-culture of tumor cells with macrophages leads to increased expression or secretion of VEGF-A from macrophages, or both. We co-cultured MDA-MB-231 tumor cells with BAC 1.2F5 macrophages labeled with CellTracker™ Green to distinguish them from cancer cells, and then stained the cells for VEGF-A. The co-culture of tumor cells with macrophages resulted in decreased intracellular VEGF-A staining in the macrophages **(Figure 3E, F)**, suggesting that tumor cells induce macrophages to secrete VEGF-A. In addition, inhibition of CSF-1R signaling (which prevented VEGF-A secretion) increased the intracellular macrophage VEGF-A in the co-culture system **(Figure 3E, F)**. In our second model using 4T1 tumor cells, we again found a decrease in intracellular VEGF-A staining in the macrophages co-cultured with cancer cells **(Supplementary Figure 1D).** The increase in macrophage VEGF-A secretion and the decrease in the intracellular VEGF-A protein levels in the macrophages were abrogated with CSF-1R neutralizing antibody as well as with the small molecule CSF-1R inhibitor, consistent to what was observed with MDA-MB-231 cells in **Figure 3**.

To determine if the VEGF-A secreted by the macrophages was due to increased VEGF-A production, we co-cultured MDA-MB-231 tumor cells with BAC1.2F5 macrophages and determined the amount of VEGF mRNA by qRT-PCR. We found that co-culture of tumor cells and

macrophages did not affect the amount of VEGF-A mRNA levels in macrophages **(Supplementary Figure 2)**. To determine the impact of CSF-1R inhibition on the levels of VEGF-A expression *in vivo*, we treated mice with either control or a CSF-1R inhibitory antibody and looked at the total level of VEGF-A (both intra- and extracellular) within TMEM doorways. We found that CSF-1R inhibition does not affect the steady state expression or stability of VEGF-A levels in the TMEM doorway. **(Figure 3G, H)**. Both findings are consistent with the observation that tumor cell secreted CSF-1 does not upregulate VEGF-A expression in macrophages **(Supplementary Figure 2)**, but rather controls VEGF-A secretion from macrophages, which is retained within the TMEM doorway. Altogether, these results indicate that tumor cells stimulate macrophages to secrete VEGF-A but have no role in inducing macrophage VEGF-A production.

Inhibition of CSF-1R reduces TMEM doorway-associated vascular opening and trans-endothelial migration

As CSF-1R signaling regulates macrophage VEGF-A secretion, and macrophage-secreted VEGF-A is required for vascular opening at TMEM doorways (10), we examined the role of CSF-1R in mediating vascular opening and tumor cell intravasation at TMEM doorways *in vivo* as defined in **Figure1** and previously (6). We injected tumor bearing PyMT mice *i.v.* with CSF-1R blocking antibodies or IgG control antibodies four hours prior to sacrifice and injected high molecular weight dextran (155 kDa) one hour before sacrifice. We stained the tumor tissue for CD31, TMR-Dextran, and ZO-1 to examine the effects of CSF1-R inhibition on TMEM doorway activity and vascular junctional integrity (**Figure 4A).** Acute inhibition of CSF-1R reduced extravascular dextran at TMEM doorways, indicating that TMEM doorways were less active when CSF-1 signaling is inhibited **(Figure 4B)**. Vascular ZO-1, a component of endothelial tight junctions that maintains vascular junction integrity, increased with inhibition of CSF-1R suggesting that the endothelial junctions were less permeable upon CSF-1 inhibition **(Figure 4C)**. To determine whether blockade of CSF-1 signaling and subsequent inhibition of TMEM doorway opening prevented tumor cells from entering the vasculature, we collected the blood of the mice during sacrifice and measured the number of circulating tumor cells (CTCs). The number of CTCs were significantly reduced upon CSF-1R inhibition **(Figure 4D)**. These results indicate that CSF-1R signaling is not only involved in tumor cell and macrophage streaming migration, as reported before (8), but also in signaling between tumor cells, macrophages, and endothelial cells, creating intravasation-associated vascular openings and allowing intravasation of tumor cells, leading to CTCs.

To further examine the effects of blocking CSF-1R signaling on macrophage-mediated transendothelial migration of tumor cells, we used our previously established *in vitro* trans-endothelial migration (iTEM) assay (34). The iTEM assay mimics the conditions seen at the TMEM doorway during intravasation (10, 32) and allows us to quantify the number of tumor cells that cross the endothelium. We have previously shown that breast tumor cells alone cross through the endothelial cell barrier poorly, but transendothelial migration is enhanced in the presence of macrophages (34, 35). As shown before, tumor cells exhibited a basal level of trans-endothelial migration, which was significantly increased in the presence of macrophages (**Figure 4E**). However, there was no enhancement of tumor cell trans-endothelial migration in presence of macrophages when CSF-1R signaling was inhibited by either a CSF-1R blocking antibody or a small molecule inhibitor of CSF-1R (GW2580) (**Figure 4E**).

To further establish that CSF-1R signaling between tumor cells and macrophages was important for enhancing tumor cell migration across the endothelial cell layer, we used BMMs lacking CSF-1R (C*sf1r-/-)* in the iTEM assay and observed no increase of transmigration of tumor cells compared to tumor cells cultured without macrophages **(Figure 4F)**. Similarly, to establish that CSF-1 secreted by tumor cells specifically is responsible for the increased trans-endothelial migration, and not the other TMEM doorway cells present in the iTEM assay, we knocked down CSF-1 in MDA-MB-231 cells (**Supplementary Figure 3**) and used these tumor cells in the iTEM assay. We found that unlike tumor cells expressing CSF-1, tumor cells with reduced CSF-1 expression did not support increased trans-endothelial migration in the presence of macrophages (**Figure 4G**). Thus, inhibition of CSF-1R signaling blocked the ability of macrophages to enhance tumor cell trans-endothelial migration.

Discussion:

It has been previously shown that TMEM doorway associated vascular opening (TAVO) requires vascular endothelial growth factor-A (VEGF-A) produced by the TMEM doorway macrophage. In particular, a TIE2^{hi}/VEGF-A^{hi} TMEM doorway-associated macrophage interacts with its associated endothelial cell through secretion of VEGF-A to mediate blood vessel opening by disrupting endothelial cell adherens and tight junctions (10). We have demonstrated, using intravital imaging, that the vascular opening in tumors is an acute, localized, and transient event, and only occurs at TMEM doorways, as opposed to VEGF-A injected into the vasculature, which caused general and continuous leakage of blood contents from all blood vessels (10). We have further shown that these TAVO events occur simultaneously with tumor cell intravasation, and are required for tumor cell intravasation. When VEGF-A is knocked out specifically in macrophages,

TAVO events are blocked, as is tumor cell intravasation (10). These observations are consistent with and provided a mechanism for the finding that the number of TMEM doorways measured by multiplex immunohistochemistry in formalin-fixed paraffin-embedded breast cancer sections is a clinically validated prognostic indicator of distant metastasis in breast cancer patients (12-14). However, the signal that triggers the secretion of VEGF-A by the TMEM doorway macrophage, the most critical step for TMEM doorway opening, has remained unknown, until now.

There is evidence of a paracrine interaction between tumor cells and macrophages, which facilitates tumor cell migration toward blood vessels in breast cancer (8, 29). This interaction is driven by a CSF-1/EGF paracrine loop, wherein tumor cells secrete CSF-1 (which attracts CSF-1R expressing macrophages), while macrophages in turn secrete EGF (which attracts EGFR-expressing tumor cells). The tumor cells respond to EGF-secreting macrophages by migrating towards them and secreting more CSF1, therefore generating a paracrine loop (8, 27, 29, 36). These signaling events create a chemotactic axis in which the CSF-1/EGF signals become amplified, allowing the tumor cells and macrophages to remain in close proximity with each other as they migrate together as cell pairs (a process called streaming (8, 27, 29, 36)). Once the tumor cells within the loop encounter an HGF signal, which is found in a gradient in the tumor microenvironment with the highest concentration near blood vessels (7), the tumor cell-macrophage pairs start migrating toward the blood vessels along the HGF gradient, adding directionality to the migrating partners **(Figure 5A)**. Once at the blood vessels, the streaming tumor cells can intravasate through active TMEM doorways, following a TAVO event (7, 10, 11). The critical role of the paracrine CSF-1/EGF loop between tumor cells and macrophages, as well as the HGF gradient and directional migration in metastasis were confirmed by genetic or pharmacological inhibition of EGF, CSF1, or the c-Met receptor (which binds HGF), which significantly impairs streaming of both tumor cells and macrophages and blocks tumor cell dissemination in *in vivo* breast cancer metastasis models (7, 8, 29, 36).

Here we demonstrate that while the TMEM doorway tumor cell and macrophage remain in direct and stable contact on the blood vessel **(Figure 5B)**, the CSF-1 signaling as observed in streaming tumor cells not on blood vessels persists between tumor cells and macrophages in the TMEM doorway on the blood vessel, resulting in localized macrophage secretion of VEGF-A. We found that TMEM doorway tumor cells secrete CSF-1 which binds to the TMEM doorway macrophages expressing CSF-1R. This event triggers localized secretion of VEGF-A by TMEM doorway macrophages and leads to downstream TAVO events, where acute vascular opening within the endothelium allows tumor cells to intravasate through the TMEM doorway and these CTCs can form distant metastases **(Figure 5C)**, which we have previously visualized and

characterized (10, 31, 37). We demonstrate in this study that inhibition of CSF-1R *in vitro* by either knocking down CSF-1R in macrophages or adding a blocking antibody decreased macrophage release of VEGF-A, and transendothelial migration of tumor cells, an *in vitro* measure of intravasation capability. *In vivo*, acute treatment of tumor bearing mice with a CSF-1R blocking antibody significantly increased vascular tight junction stability, decreased TMEM doorway activity and TAVO events, as well as formation of CTCs. We did not detect a difference in VEGF-A expression around the TMEM doorway when a CSF-1R blocking antibody was used *in vivo* (Figure 4G, 4H). This is consistent with our finding that CSF-1 signaling does not increase the expression of VEGF-A in the TMEM doorway macrophage, but rather triggers the local secretion of VEGF-A from the TMEM doorway macrophage, where it binds to and signals to the nearby TMEM doorway endothelial cell. Therefore, in the absence of CSF-1 secretion by the TMEM doorway tumor cell, the VEGF-A is retained within the TMEM doorway macrophage, the blood vessel near the TMEM doorway remains impermeable and tumor cells are unable to intravasate through TMEM doorways.

The importance of this study beyond the primary tumor is emphasized by the finding that TMEM doorways are found not only in invasive ductal breast carcinomas, but also in metastatic foci in lymph nodes (18, 19) and lungs (6). We and others have found that secondary metastases can seed tertiary metastases (1-4), and presence of TMEM doorways at secondary sites may perpetuate metastatic dissemination **(Figure 5D)** even after removal of the primary tumor. Importantly, blocking the function of TMEM doorways could not only prevent the dissemination of cancer cells from primary tumors, but also prevent re-dissemination of tumor cells from metastatic sites, which may occur after the resection of primary tumors (10, 11, 38, 39). Therefore, even if the tumors are highly metastatic, we may be able to increase patient survival or quality of life, or both, by blocking TMEM doorway function systemically, which would lessen overall metastatic burden. Inhibition of both Tie2 and CSF-1 signaling to prevent TAVO events (10, 31), along with standard of care therapies, might be an effective way to prevent re-dissemination from both primary and metastatic tumor sites, and allow for better patient survival.

While we have previously shown in mice that transient, short-term blockade of VEGF-A expression in macrophages is effective in inhibiting TMEM doorway activity, TAVO events, and formation of CTCs (10), patients treated with anti-angiogenic therapies targeting VEGF-A (e.g., bevacizumab and other VEGF-A inhibitors) eventually develop therapeutic resistance (40). One mechanism of tumor resistance or recurrence following anti-angiogenic therapy in patients is attributed to the increased recruitment and infiltration of Tie2-expressing macrophages into the tumor in response to apoptosis, necrosis, and hypoxia after vascular regression (40). Additionally,

the ligand for Tie2, Ang2, is upregulated in response to hypoxic conditions. Tie2-Ang2 signaling can function in a similar manner to VEGF-A signaling to promote tumor angiogenesis, bypassing VEGF-A inhibition, and even being enhanced by such inhibition. As such, Tie2 is an attractive pharmacological target for the suppression of tumor angiogenesis and tumor cell dissemination. We have found that TMEM doorway macrophages are also characterized by expression of Tie2 (10) and that a selective inhibitor of Tie2, rebastinib, inhibits TMEM doorway activity, formation of CTCs, and metastasis in several mouse models of metastasis and patient derived xenografts (32). The mechanism of how Tie2 contributes to signaling between the TMEM doorway cells to mediate the TAVO events is still unclear and warrants further investigation. Uncovering the complete mechanism of TMEM doorway opening in primary and secondary sites is critical. We expect that inhibiting TAVO events will be have a great impact on our ability to increase the survival of both patients with metastatic disease and patients who are likely to develop metastatic disease.

Materials and Methods:

Cell culture. MDA-MB-231 were cultured in Dulbecco's Modified Eagle Medium (DMEM) (cat# SH30243, Hyclone, GE Healthcare Life Sciences, Logan, Utah, USA) supplemented with 10% fetal bovine serum (cat# S11550, Atlanta Biologicals, Flowery Branch, GA, USA). BAC 1.2F5 macrophages (41) and bone marrow derived macrophages (BMMs) were cultured in Minimum Essential Medium, Alpha (α-MEM) (cat# 15-012-CV, Corning, Tewksbury, MA, USA) supplemented with 10% fetal bovine serum (cat# 100-106, Gemini Bio-Products, Sacramento, CA, USA) and 36 µg/mL CSF-1 (a gift from Dr. Richard Stanley). Human Umbilical Vein Endothelial Cells were cultured in EGM-2 media (cat# CC-3162, Lonza, Allendale, NJ, USA) according to the manufacturer's instructions and not used beyond passage 5 for any experiments.

Mice. All studies involving mice were carried out in accordance with the National Institutes of Health regulation concerning the care and use of experimental animals. The procedures used were approved by the Albert Einstein College of Medicine Animal Care and Use Committee. Transgenic mice expressing the Polyoma Middle T (PyMT) oncogene under the control of the mammary tumor virus long terminal repeat (MMTV-LTR) were bred in house.

Inhibitors. Inhibitors were administered based on established doses of efficacy in previous studies. Animals were treated with 2.5 µg of anti-CSF-1R neutralizing antibody (clone AFS98, Novus Biologicals), or antibody isotype control was administered by tail vein *i.v.* 4 h before

termination of the experiment as previously described (27). For *in vitro* studies, GW2580 a small molecule inhibitor of CSF-1R (LC Laboratories) was dissolved in DMSO was used at a concentration of 100 nM, and anti-CSF-1R neutralizing antibody (clone AFS98, Novus Biologicals) was used at a concentration of 50ng/mL.

Immunofluorescent labeling of tumor vasculature and extravasation with 155 kDa dextran-TMR. Labeling flowing vasculature and sites of permeability was performed as previously described (10). Briefly, to quantify extravasation high molecular weight 155 kDa TMR-dextran diluted in PBS was administered by tail vein *i.v.* one hour before the termination of the experiments. Anti-mouse CD31-biotin was administered by tail vein *i.v.* 10 minutes before the end of the experiment to label flowing blood vessels. At time of sacrifice tumors were removed and fixed for 48 hrs in 10 % formalin in a volume ratio of tumor to formalin of 1:7 and made into paraffin blocks. 5 µm sections of tumors were cut and immunofluorescence performed.

Immunofluorescence staining of tissue. Tumor sections were dewaxed in acetone and rehydrated in alcohol followed by water. Antigen retrieval was performed with a citrate solution at pH 5.5 in a humidified chamber. The slides were washed with PBS-T (0.1% tween) and blocked with block solution (2% BSA, 10 % FBS in PBS). One 5 µm section from each tumor was stained for hematoxylin and eosin (H&E) and one for TMEM doorway. TMEM doorway stain is a triple immuno-stain for predicting metastatic risk, in which 3 antibodies are applied sequentially and developed separately with different chromogens on a Dako Autostainer. The following primary antibodies were used for immunostaining of TMEM: mouse anti-Mena (BD Bioscience), rabbit anti-CD31 (77699s; Cell Signaling Technology), rabbit anti-Iba-1 (FUJIfilm, Wako biosciences). The sequential tissue sections were stained with: rat anti-endomucin, Red Fluorochrome 635-conjugated anti-Iba-1 (FUJIfilm, Wako biosciences), rat anti-VEGF (clone 2G11-2A05, Biolegend), Alexa 555-conjugated rabbit anti-CSF-1 (Bioss Inc), rat anti-mouse CD68 (clone FA-11, Serotec), and goat anti-MRC1/CD206 (R&D Systems). Sections were washed with PBS-T and the primary antibodies were detected with AlexaFluor 488, 555 or 647 secondary antibody conjugates (Molecular Probes/Invitrogen) as needed and nuclei stained with 4, 6-diamidino-2-phenylindole (DAPI). All fluorescently labeled samples were mounted with Prolong Diamond antifade reagent (Molecular Probes/Invitrogen) and imaged with a digital whole slide scanner (3D Histech; 20X objective). Images of tumor sections were acquired using mosaic tiling (15 % overlap) and reconstructed into a single image in CaseViewer. Individual fields of view images

were imported into ImageJ or VisioPharm for analysis. TMEM doorways were identified as previously described (10, 13, 14). Vascular junctions and extravascular dextran were quantified as previously described (10, 30). Briefly, the CD31 channel (blood vessel), dextran and vascular junction (ZO-1) were each thresholded to just above background based upon intensity. The extravascular dextran area was isolated by subtracting the blood vessel mask from the dextran mask. The remaining extravascular dextran area and blood vessel area were then measured.

Extravascular dextran and intracellular CSF-1 in the TMEM tumor cell. To identify active TMEM doorways, we utilized an improved and automated method of a prior TMEM activity assay that takes into account the presence of high-molecular weight dextran that leaks into the tissue, as a result of TMEM-associated vascular opening (10, 30, 31). The algorithmic improvement of this assay involves the automated measurement of the entire tumor as a single region of interest (ROI), instead of selecting a definite number of high power fields as ROIs, thus providing a more accurate representation of the entire tumor, minimizing operator-dependent biases, and significantly increasing the logistic capacity of the analysis.

In short, serial tissue sections were cut and stained for Dextran, CSF-1, and Endomucin by IF (Section 1) and for Iba1, Endomucin, and panMena (Section 2). The sections were then imaged with a digital whole slide scanner and aligned to the single cell level using the TissueAlign module in Vis (Visiopharm, Hoersholm, Denmark). IF images were thresholding above background, creating binary masks for endomucin (blood vessel) and dextran signals. These masks were then superimposed so as to be able to differentiate between intravascular and extravascular dextran signal. In the IHC section, TMEM doorways were identified using previously published criteria (13, 14). In this manner, the amount of extravascular dextran around TMEM doorways could be quantified. For quantification of intracellular CSF-1, the TMEM doorway associated tumor cell was manually identified using the Mena stain in IHC section and a mask manually created. CSF-1 was then quantified in this mask.

siRNA knockdown. MDA-MB-231 cells were transfected with Stealth siRNAs HSS102355, HSS102356, HSS175321 to CSF-1 (Thermo Fisher Scientific, Waltham, MA) at a concentration of 200 pmols with use of Lipofectamine 2000 reagent (Invitrogen, Carlsbad, CA).

Immunofluorescence staining of cells. Macrophages were either expressing GFP or labelled

with CellTracker Green™ dye prior to start of the co-culture of mono-culture VEGF IF experiments. 100,000 macrophages were used in the experiments. The tumor cells were co-cultured together or macrophages were cultured alone as per the experiment or stimulated with CSF-1 for the amount of time mentioned in the figure legends. The experiments were stopped by washing the cells with ice-cold PBS followed by fixing them for 20min in 4% PFA, and permeablizing them in 0.1%triton in PBS. The cells were stained for VEGF-A using Ab against VEGF-A and anti-rat 647 secondary Ab. The amount of VEGF-A in the macrophage was measured by first outlining the macrophages in the green (488) channel in ImageJ/Fiji (42) and using that outline in the far-red (647) channel to measure the VEGF signal within the macrophage.

Quantitative real-time polymerase chain reaction. To quantify gene expression, cells were grown under normal culture conditions. Total RNA was isolated from cells by using the RNeasy plus mini kit (Perkin Elmer) and cDNA was synthesized and amplified from total RNA using the using SuperScript IV VILO Master Mix w/ ezDNase enzyme (Thermo Fisher Scientific, Cat.No.:11766050) as per manufacturers protocol. Baseline expression was measured using a SYBR Green Mastermix (Thermo Fisher Scientific, Cat.No.:4367659) as per the manufacturers protocol and the reaction ran using QuantStudio3 system (Thermo Fisher Scientific).

For the co-culture assay, species specific probes and primers were used to perform real-time PCR, with each reaction being done in triplicate. The mean cycle threshold (Ct) values were then used to analyze relative expression. Analysis was done using the ΔΔCt method in which all Ct values were normalized to GAPDH. The table below lists the primers used for the qPCR reaction.

Gene	**Forward**	**Reverse**
mGAPDH	CTC ATG ACC ACA GTC CAT GC	CAC ATT GGG GGT AGG AAC AC
mVEGF	AGC AGA AGT CCC ATG AAG TGA	ATG TCC ACC AGG GTC TCA AT
hGAPDH	CTCCTGTTCGACAGTCAGCC	ACCAAATCCGTTGACTCCGAC

hβ-Actin	CTTCGCGGGCGACGATGC	CGTACATGGCTGGGGTGTTG
hCSF-1	CCTCCCACGACATGGCT	GAGACTGCAGGTGTCCACTC

ELISA. 1 X 10^6 BAC macrophages were cultured alone or co-cultured with 1 X 10^6 MDA-MB 231 tumor cells for up to 48 hours in complete DMEM media with 300units/mL of CSF-1, or with 1 X 10^6 HUVECs which were allowed to form a monolayer overnight and macrophages added over the monolayer for 45mins in □-MEM media with 300units/mL of CSF-1. Media from the cultured cells were collected at the indicated time points and stored into -80^0C until use. ELISA was performed as per the manufacturer's recommendation using the mouse VEGF DuoSet ELISA kit from R&D Systems. The amount of VEGF secreted by macrophages was interpolated from the measurements of the standard curve.

Transendothelial Migration Assay (iTEM assay). The transendothelial migration assay was performed as previously described (34, 43, 44) and briefly described here. The transwell was prepared so that tumor cell transendothelial migration was in the intravasation direction (from subluminal side to luminal side of the endothelium). To prepare the endothelial monolayer, the underside of each transwell (8µm pore size) were coated with 50 µL of Matrigel (2.5 µg/mL; Invitrogen). Approximately 100,000 HUVEC cells were plated on the Matrigel coated underside of the transwells. Transwells were then flipped into a 24-well plate containing 200 µL of EGM-2 and monolayers were formed over a 48-hour period. The integrity of the endothelium was measured using low molecular weight dextran as described previously (44). Macrophages and tumor cells were labelled with cell tracker dyes (CMFDA, CMPTX respectively, from Invitrogen, Carlsbad, CA, USA) before the experiment. Then, 15,000 tumor cells and 60,000 macrophages were added to the upper chamber in 200µL of DMEM supplemented without serum while the bottom chamber contained EGM-2 supplemented with 36µg/mL of CSF-1. After 18 hours, the tranwells were fixed and stained for ZO-1 as previously described. Transwells were imaged using a Leica SP5 confocal microscope using a 60x 1.4NA objective and processed using ImageJ/Fiji (42). Quantitation was performed by counting the number of tumor cells that had crossed the endothelium within the same field of view (60X, 10 random fields) and represented as normalized values from at least 3 independent experiments.

Statistical analysis. Individual animals in each cohort are presented as individual points on a dot plot. A horizontal line indicates the mean value and the error bars represent the standard error of the mean. Statistical significance was determined by the comparison of the means of two groups using an unpaired, two-sided *t*-test using Prism (Graph Pad Inc.). Data sets were checked for normality (D'Agostino & Pearson omnibus normality test or Shapiro-Wilk normality test) and unequal variance using Prism (Graph Pad Inc.). Welch's correction was applied to *t*-tests as needed. *P* values of less than 0.05 were deemed significant. For *in vitro* experiments results are representative of at least three independent experiments. Statistical analysis was performed using an unpaired two-tailed Student's *t*-test, or ANOVA as indicated.

Acknowledgments:

This work was supported by the NCI grants (R01 CA255153, PPG CA257885, R01 CA240646, F32 CA243350, K99 CA237851), SIG OD019961, the Gruss-Lipper Biophotonics Center, the Integrated Imaging Program, the Integrated Imaging Program for Cancer Research, The Evelyn Gruss-Lipper Charitable Foundation, and The Helen & Irving Spatz Foundation. We would like to thank the Analytical Imaging Facility at Albert Einstein College of Medicine for imaging support.

Figure Legends:

Figure 1. TMEM doorway tumor cells show increased CSF-1 levels at active TMEM doorways. A) Cartoon denoting the identification of parameters used for analysis of CSF-1 levels in TMEM doorway tumor cells (TTCs) and TMEM doorway function. The three cells composing the TMEM doorway are indicated by the yellow triangle connecting the TMEM doorway macrophage (TM), the TMEM doorway endothelial cell (TEC) and the TTC. Intravascular dextran is in the lumen of blood vessel, extravascular dextran is outside the lumen of blood vessel, and CSF-1 is directly measured in the TTC. **B)** Panel shows inactive and active TMEM doorways, visualized by immunohistochemistry (IHC) staining for Mena, Iba-1, and endomucin. The three cells of the TMEM doorway (contained in black circle, with the three cells forming the TMEM doorway indicated with the yellow triangle) are the TMEM doorway endothelial cell (TEC, endomucin stained in blue, circled in white), TMEM doorway macrophage (TM, Iba1 stained in brown, circled in teal), and TMEM doorway tumor cell (TTC, Mena stained in pink, and circled in pink) and black arrows indicate where the cells are localized within the TMEM doorway. TMEM doorways were identified using automated analysis by VisioPharm identifying three adjacent immuno-histochemical stains. **C)** The sequential tissue section after the IHC in (B) was stained

with immunofluorescence (IF) with antibodies against endomucin (white), dextran (green), CSF-1 (red), and nuclear stain DAPI (blue). The two sequential sections from 1B and 1C were aligned and the same TMEM doorways were matched between the two sections, as indicated by the black circle in the IHC panel (1B) and white circle in the IF panels (1C) showing the same TMEM doorway after alignment. The panel demonstrates the association of CSF-1 level in the TMEM doorway tumor cell (TTC) and TMEM doorway activity. The middle panel shows the extravascular signal for dextran as a green mask and the endomucin stain as a white mask, where thresholded, positive signal for these stains was converted into a binary mask. Active versus inactive TMEM doorways were distinguished by the presence of extravascular dextran staining non-overlapping with the endomucin stain, which indicates that the vessel had a TMEM doorway-associated vascular opening (TAVO). Scale bars=20μm. **D)** Immunofluorescence measurement of CSF-1 levels in TMEM doorway tumor cells in active and inactive TMEM doorways. TMEM doorways were identified in the IF-stained sections as described above. Active TMEM doorways were identified by the presence of extravascular dextran which is not present in inactive TMEM doorways (see panel C). Next, tumor cells were identified using the Mena positive cells at TMEM doorway (panel 1B, IHC stain). The level of CSF-1 in the TMEM doorway tumor cells was measured in both active and inactive TMEM doorways using Visiopharm. n= 12 mice. ****$P < 0.0001$ analyzed by t-test.

Fig. 2 TMEM doorway macrophages express CSF-1R and tumor cells secrete CSF-1. A) VEGF ELISA of conditioned media obtained from BAC1.2F5 macrophages (Mϕ) with CSF-1 (3000units/mL) for the times indicated. VEGF is indicated as absolute amount (pg/ml) of secreted protein. n=3 individual experiments done in duplicate, *p<0.05, by two-way ANOVA. **B)** CSF-1 ELISA of conditioned media obtained from MDA-MB 231 tumor cells (TC). TCs were cultured for 24 hours in serum-free media and amount of CSF-1 secreted by the TCs measured in the tumor cell conditioned media by ELISA. Control is media not exposed to tumor cells but treated the same way as the cells. CSF1 secreted is denoted in absolute amount (pg/mL) of secreted protein. n=3 individual experiments done in duplicate. *p<0.05 ****p<0.0001 by two-way ANOVA. **C)** Immunofluorescence staining and quantification of PyMT tumor sections stained for CSF-1R (green), vasculature (CD31, magenta), TMEM doorway macrophages (CD206, red) and DAPI (blue). The cells composing a TMEM doorway, identified as described in Fig 1 (10), are indicated by the points of the yellow triangle being the relative positions of the TMEM doorway endothelial cell (TEC, white circle), TMEM doorway macrophage (TM, blue circle) and TMEM doorway tumor cell (TTC, pink circle) indicated with white arrows. Scale bar

50 µm. **D)** Quantification of the percent of CD68+ TMEM doorway macrophages and CD206+ TMEM doorway macrophages which stain positively for CSF-1R (*n* = 6).

Figure 3. Tumor cell secreted CSF-1 increases CSF1-R dependent macrophage VEGF secretion. A) VEGF ELISA of conditioned media obtained from macrophages (BAC1.2F5) co-cultured with MDA-MB-231 tumor cells treated with control antibody (ctrl Ab), CSF-1R blocking Ab or CSF-1R inhibitor (GW2580), denoted in absolute amount (pg/mL) of secreted protein. n=3 individual experiments done in duplicate, *p<0.05, ***p<0.001, ****p<0.0001 analyzed by two-way ANOVA. **B)** VEGF ELISA of conditioned media obtained from macrophages (BAC1.2F5) cultured in conditioned media from MDA-MB-231 tumor cells and treated with control Ab, CSF-1R blocking Ab (CSF-1R Ab) or CSF-1R inhibitor (GW2580), denoted in absolute amount (pg/mL) of secreted protein. n=3 individual experiments done in duplicate, *p<0.05, **p<0.01, ****p<0.0001 analyzed by two-way ANOVA. **C)** VEGF ELISA of conditioned media obtained from bone marrow macrophage (BMMs) either expressing or lacking CSF-1R co-cultured with MDA-MB-231 tumor cells for the times indicated. VEGF levels are denoted in absolute amount (pg/mL) of secreted protein. n=3 individual experiments done in duplicate, ****p<0.0001 analyzed by two-way ANOVA. **D)** VEGF ELISA of conditioned media obtained from BMMs either expressing or lacking CSF-1R cultured in conditioned media from MDA-MB-231 tumor cells for the times indicated. VEFG levels are denoted in absolute amount (pg/mL) of secreted protein. n=3 individual experiments done in duplicate, ****p<0.0001 analyzed by two-way ANOVA. **E)** Immunofluorescence staining of VEGF in macrophages (labelled with CellTracker™ Green) cultured with or without tumor cells (labelled with CellTracker™ Red) and treated with either ctrl Ab or CSF-1R blocking Ab. Scale bar 5 µm. **F)** Quantitation of the VEGF fluorescence intensity in macrophages in E. The amount of VEGF in the macrophage was quantified using ImageJ. n=3. *p<0.05, **p<0.01, ****p<0.0001 analyzed by two-way ANOVA. **G, H)** Immuno-staining and quantification of VEGF intensity around TMEM doorways, obtained from PyMT mice treated with control antibody (ctrl Ab) or CSF-1R blocking Ab. Sequential tumor sections derived from PyMT tumors were stained by immunofluorescence (VEGF, Iba-1) and IHC (TMEM doorways-Mena, Iba-1, endomucin). TMEM doorways were identified as described in figure 1A. The circle in the IHC (black) and IF (white) panels show the same TMEM doorways obtained from the alignment of serial sections, and the three cells making up the TMEM doorway are pointed out with the yellow triangle in each panel. TMEM doorways are outlined in the circle with the endothelial cell (TE, blue stain, white circle), macrophage (TM, brown stain, teal circle) and TMEM doorway tumor cell (TTC, pink stain, pink circle) indicated with

arrows. Next, the two sequential sections were aligned and TMEM doorway was identified in the IF-stained section. The immunofluorescence intensity of VEGF-A expression (green stain) in the identified TMEM doorway ROIs was measured and plotted here. N=analysis of images obtained from tissue sections from individual 11 mice, Scale bar 20 µm, not significant, analyzed by t-test.

Figure 4. Inhibition of CSF-1R signaling reduces TMEM doorway associated vascular opening (TAVO) and trans-endothelial migration. A) IF staining of tumor tissue from mice treated with control Ab or CSF-1R Ab were stained for CD31 (green), TMR-dextran (red), and ZO-1 (magenta). Right panel shows increased magnification of yellow box from middle panel to demonstrate overlap between CD31 and ZO-1 stains (merge/overlap indicated with white signal, and pointed out with white arrows). **B)** Quantification of extravascular 155 kDa dextran-TMR (*, $P = 0.0247$), **C**) Vascular ZO-1 (*, $P = 0.00366$), and **D**) circulating tumor cells (A, B, C $n = 8$) for mice treated with control Ab or CSF-1R blocking Ab in A). *p<0.05, analyzed by t-test. **E)** Quantitation of subluminal to luminal trans-endothelial migration (iTEM activity, which is a measure of number of intravasating cells in the intravasation direction) of MDA-MB-231 cells plated on the confluent and sealed endothelium either alone or with BAC1.2F5 macrophages. Tumor cells were treated with control antibody (ctrl Ab & DMSO), CSF-1R blocking Ab (CSF1R Ab) or CSF-1R inhibitor (GW2580). Tumor cells were labelled with CellTracker™ green which allowed us to identify and quantify the cells crossing. The number of MDA-MB-231 cells which crossed the endothelium were imaged using a confocal microscope and quantified using ImageJ software. N=3, $^{**}P < 0.01$ analyzed by two-way ANOVA. **F)** Quantitation of iTEM activity of MDA-MB-231 cells plated on the endothelium alone or with BMMs expressing or lacking CSF-1R expression. Tumor cells were labelled with CellTracker™ green which allowed us to identify and quantify the cells crossing. The number of MDA-MB-231 cells which crossed the endothelium were imaged using a confocal microscope and quantified using ImageJ software. N=3, $^{***}P < 0.001$ analyzed by two-way ANOVA. **G)** Quantitation of iTEM activity of MDA-MB-231 cells transfected with either control siRNA or 3 different siRNAs targeting CSF-1 (#1, #2, #3) and were plated on the endothelium either alone or with BAC1.2F5 macrophages. Tumor cells were labelled with CellTracker™ green which allowed us to identify and quantify the cells crossing. The number of MDA-MB-231 cells which crossed the endothelium were imaged using a confocal microscope and quantified using ImageJ software. n=3, $^{***}P < 0.001$ analyzed by two-way ANOVA.

Figure 5. Model of CSF1-induced TMEM doorway opening and release of CTCs into the blood stream. A) In the primary tumor, macrophages and tumor cells exhibit a CSF1-EGF

paracrine interaction between tumor cells and macrophages which facilitates tumor cell migration toward blood vessels in breast cancer. Tumor cells secrete CSF-1 which attracts CSF-R1 expressing macrophages, which in turn secrete EGF, increasing the migration of EGFR-expressing tumor cells. The tumor cells within the loop encounter a HGF signal found in a gradient in the tumor microenvironment with the highest concentration near blood vessels. The tumor cells will migrate toward the blood vessels along the HGF gradient, adding directionality to the migration of the tumor cell-macrophage paracrine loop engaged partners. **B)** In an inactive TMEM doorway (box), with the absence of any CSF1 secreted by the TMEM doorway tumor cell (TTC), the VEGF-A remains within the TMEM doorway macrophage (TM). The blood vessels, including the TMEM doorway endothelial cell (TEC) within the tumor remain sealed and do not allow tumor cells to intravasate through TMEM doorways. **C)** In contrast, in an active TMEM doorway, CSF-1 is secreted by the TMEM doorway tumor cell and binds to macrophage CSF-1R, stimulating the TMEM doorway macrophage to secrete its VEGF. VEGF causes vascular opening (TAVO event) and allows tumor cells to intravasate through the TMEM doorway, creating CTCs, and dextran or blood to leak out of the vessel. **D)** These circulating tumor cells (CTCs) travel through the vasculature to secondary sites where TMEM doorways are also found in metastatic foci in lymph nodes and lungs. Thin membranous connections between macrophages and tumor cells stretch from the macrophage on extravascular side of the blood vessel through the endothelial junctions and interact with CTCs which could facilitate CTC extravasation at secondary sites. TMEM doorways in metastases could also be the sites were tumor cells re-intravasate and then seed tertiary metastases.

Supplementary Fig. 1 CSF-1 is required for bone marrow derived macrophage VEGF secretion and tumor cell secreted CSF-1 increases macrophage VEGF secretion. A) VEGF ELISA of conditioned media obtained from macrophages (BMMs) co-cultured with or without tumor cells (MDA-MB 231), in presence of CSF-1R small molecule inhibitor (GW2580) or vehicle, and VEGF ELISA of conditioned media obtained from macrophages (BMMs) cultured in conditioned media obtained from tumor cells (CM), in presence of CSF-1R small molecule inhibitor (GW2580) or vehicle, denoted in absolute amount (pg/mL) of secreted protein. n=3 individual experiments done in duplicate, ****$p<0.0001$ by two-way ANOVA. **B)** CSF-1 ELISA of conditioned media obtained from 4T1 tumor cells. n=3, *$p<0.05$, analyzed by t-test. **C)** VEGF ELISA of conditioned media obtained from macrophages (BAC1.2F5) co-cultured with 4T1 tumor cells treated with control (ctrl) antibody (Ab), CSF-1R blocking Ab or CSF-1R inhibitor (GW2580), denoted in absolute amount (pg/mL) of secreted protein. n=2 individual experiments done in

duplicate, *p<0.05, **p<0.01 ***p<0.001 analyzed by two-way ANOVA. **D)** Tumor cells decrease intra-cellular macrophage VEGF. Quantification of the immunofluorescence staining intensity of VEGF in macrophages (labelled with CellTracker™ Green) cultured with or without tumor cells 4T1 (labelled with CellTracker™ Red) and treated with either ctrl Ab or CSF-1R blocking Ab. Macrophages were labeled with CellTracker™ Green to distinguish them from tumor cells. The amount of VEGF in the macrophage was quantified using ImageJ. n=3. ****p<0.0001 analyzed by two-way ANOVA.

Supplementary Figure 2: CSF-1 secreted by tumor cells does not increase macrophage VEGF mRNA levels. qRT PCR determining the VEGF-A mRNA levels using VEGF-A primers or control primers (GAPDH) in macrophages (BAC1.2F5) cultured alone or with tumor cells (MDA-MB 231). n=3 individual experiments done in triplicate, non-significant, analyzed by student's t-test.

Supplementary Figure 3: CSF-1 knock-down in MDA-MB-231 cells. qRT PCR determining the CSF-1 mRNA levels in MDA-MB-231 cells transfected using Lipofectamine 2000 with ctrl siRNA or 3 different CSF-1 siRNAs (#1, #2, #3) for 48hrs. n=3 individual experiments done in duplicate, ***p<0.001, ****p<0.0001 analyzed by two-way ANOVA.

REFERENCES

1. Borriello L, Condeelis J, Entenberg D, Oktay MH. Breast Cancer Cell Re-Dissemination from Lung Metastases-A Mechanism for Enhancing Metastatic Burden. J Clin Med. 2021;10(11).
2. Kim MY, Oskarsson T, Acharyya S, Nguyen DX, Zhang XH, Norton L, et al. Tumor self-seeding by circulating cancer cells. Cell. 2009;139(7):1315-26.
3. Chaffer CL, Weinberg RA. A perspective on cancer cell metastasis. Science. 2011;331(6024):1559-64.
4. Zhang W, Bado IL, Hu J, Wan YW, Wu L, Wang H, et al. The bone microenvironment invigorates metastatic seeds for further dissemination. Cell. 2021;184(9):2471-86.e20.
5. Quail DF, Joyce JA. Microenvironmental regulation of tumor progression and metastasis. Nat Med. 2013;19(11):1423-37.
6. Condeelis J, Pollard JW. Macrophages: obligate partners for tumor cell migration, invasion, and metastasis. Cell. 2006;124(2):263-6.
7. Leung E, Xue A, Wang Y, Rougerie P, Sharma VP, Eddy R, et al. Blood vessel endothelium-directed tumor cell streaming in breast tumors requires the HGF/C-Met signaling pathway. Oncogene. 2017;36(19):2680-92.
8. Wyckoff J, Wang W, Lin EY, Wang Y, Pixley F, Stanley ER, et al. A paracrine loop between tumor cells and macrophages is required for tumor cell migration in mammary tumors. Cancer Res. 2004;64(19):7022-9.
9. Borriello L, Karagiannis GS, Duran CL, Coste A, Oktay MH, Entenberg D, et al. The role of the tumor microenvironment in tumor cell intravasation and dissemination. Eur J Cell Biol. 2020;99(6):151098.
10. Harney AS, Arwert EN, Entenberg D, Wang Y, Guo P, Qian BZ, et al. Real-Time Imaging Reveals Local, Transient Vascular Permeability, and Tumor Cell Intravasation Stimulated by TIE2hi Macrophage-Derived VEGFA. Cancer Discov. 2015;5(9):932-43.
11. Wyckoff JB, Wang Y, Lin EY, Li JF, Goswami S, Stanley ER, et al. Direct visualization of macrophage-assisted tumor cell intravasation in mammary tumors. Cancer Res. 2007;67(6):2649-56.
12. Sparano JA, Gray R, Oktay MH, Entenberg D, Rohan T, Xue X, et al. A metastasis biomarker (MetaSite Breast Score) is associated with distant recurrence in hormone receptor-positive, HER2-negative early-stage breast cancer. NPJ Breast Cancer. 2017;3:42.
13. Robinson BD, Sica GL, Liu YF, Rohan TE, Gertler FB, Condeelis JS, et al. Tumor microenvironment of metastasis in human breast carcinoma: a potential prognostic marker linked to hematogenous dissemination. Clinical Cancer Research 2009;15(7):2433-41.
14. Rohan TE, Xue X, Lin HM, D'Alfonso TM, Ginter PS, Oktay MH, et al. Tumor microenvironment of metastasis and risk of distant metastasis of breast cancer. J Natl Cancer Inst. 2014;106(8).
15. Kim G, Karadal-Ferrena B, Qin J, Sharma VP, Oktay IS, Lin Y, et al. Racial disparity in tumor microenvironment and distant recurrence in residual breast cancer after neoadjuvant chemotherapy. NPJ Breast Cancer. 2023;9(1):52.
16. Kim G, Pastoriza JM, Qin J, Lin J, Karagiannis GS, Condeelis JS, et al. Racial disparity in distant recurrence-free survival in patients with localized breast cancer: A pooled analysis of National Surgical Adjuvant Breast and Bowel Project trials. Cancer. 2022;128(14):2728-35.
17. Albain KS, de la Garza Salazar J, Pienkowski T, Aapro M, Bergh J, Caleffi M, et al. Reducing the global breast cancer burden: the importance of patterns of care research. Clin Breast Cancer. 2005;6(5):412-20.
18. Ginter PS, Karagiannis GS, Entenberg D, Lin Y, Condeelis J, Jones JG, et al. Tumor Microenvironment of Metastasis (TMEM) Doorways Are Restricted to the Blood Vessel

Endothelium in Both Primary Breast Cancers and Their Lymph Node Metastases. Cancers (Basel). 2019;11(10):1507.
19. Coste A, Karagiannis GS, Wang Y, Xue EA, Lin Y, Skobe M, et al. Hematogenous Dissemination of Breast Cancer Cells From Lymph Nodes Is Mediated by Tumor MicroEnvironment of Metastasis Doorways. Front Oncol. 2020;10:571100.
20. Entenberg D, Pastoriza JM, Oktay MH, Voiculescu S, Wang Y, Sosa MS, et al. Time-lapsed, large-volume, high-resolution intravital imaging for tissue-wide analysis of single cell dynamics. Methods. 2017;128:65-77.
21. Linde N, Casanova-Acebes M, Sosa MS, Mortha A, Rahman A, Farias E, et al. Macrophages orchestrate breast cancer early dissemination and metastasis. Nat Commun. 2018;9(1):21.
22. Harney AS, Wang Y, Condeelis JS, Entenberg D. Extended Time-lapse Intravital Imaging of Real-time Multicellular Dynamics in the Tumor Microenvironment. J Vis Exp. 2016(112):e54042.
23. Karagiannis GS, Goswami S, Jones JG, Oktay MH, Condeelis JS. Signatures of breast cancer metastasis at a glance. J Cell Sci. 2016;129(9):1751-8.
24. Entenberg D, Voiculescu S, Guo P, Borriello L, Wang Y, Karagiannis GS, et al. A permanent window for the murine lung enables high-resolution imaging of cancer metastasis. Nat Methods. 2018;15(1):73-80.
25. Curry JM, Eubank TD, Roberts RD, Wang Y, Pore N, Maity A, et al. M-CSF signals through the MAPK/ERK pathway via Sp1 to induce VEGF production and induces angiogenesis in vivo. PLoS One. 2008;3(10):e3405.
26. Eubank TD, Galloway M, Montague CM, Waldman WJ, Marsh CB. M-CSF induces vascular endothelial growth factor production and angiogenic activity from human monocytes. Journal of immunology (Baltimore, Md : 1950). 2003;171(5):2637-43.
27. Patsialou A, Wyckoff J, Wang Y, Goswami S, Stanley ER, Condeelis JS. Invasion of human breast cancer cells in vivo requires both paracrine and autocrine loops involving the colony-stimulating factor-1 receptor. Cancer Res. 2009;69(24):9498-506.
28. Hernandez L, Smirnova T, Kedrin D, Wyckoff J, Zhu L, Stanley ER, et al. The EGF/CSF-1 paracrine invasion loop can be triggered by heregulin beta1 and CXCL12. Cancer Res. 2009;69(7):3221-7.
29. Goswami S, Sahai E, Wyckoff JB, Cammer M, Cox D, Pixley FJ, et al. Macrophages promote the invasion of breast carcinoma cells via a colony-stimulating factor-1/epidermal growth factor paracrine loop. Cancer Res. 2005;65(12):5278-83.
30. Karagiannis GS, Pastoriza JM, Borriello L, Jafari R, Coste A, Condeelis JS, et al. Assessing Tumor Microenvironment of Metastasis Doorway-Mediated Vascular Permeability Associated with Cancer Cell Dissemination using Intravital Imaging and Fixed Tissue Analysis. J Vis Exp. 2019(148).
31. Karagiannis GS, Pastoriza JM, Wang Y, Harney AS, Entenberg D, Pignatelli J, et al. Neoadjuvant chemotherapy induces breast cancer metastasis through a TMEM-mediated mechanism. Sci Transl Med. 2017;9(397).
32. Harney AS, Karagiannis GS, Pignatelli J, Smith BD, Kadioglu E, Wise SC, et al. The Selective Tie2 Inhibitor Rebastinib Blocks Recruitment and Function of Tie2(Hi) Macrophages in Breast Cancer and Pancreatic Neuroendocrine Tumors. Mol Cancer Ther. 2017;16(11):2486-501.
33. Yu W, Chen J, Xiong Y, Pixley FJ, Dai XM, Yeung YG, et al. CSF-1 receptor structure/function in MacCsf1r-/- macrophages: regulation of proliferation, differentiation, and morphology. J Leukoc Biol. 2008;84(3):852-63.
34. Roh-Johnson M, Bravo-Cordero JJ, Patsialou A, Sharma VP, Guo P, Liu H, et al. Macrophage contact induces RhoA GTPase signaling to trigger tumor cell intravasation. Oncogene. 2014;33(33):4203-12.

35. Pignatelli J, Bravo-Cordero JJ, Roh-Johnson M, Gandhi SJ, Wang Y, Chen X, et al. Macrophage-dependent tumor cell transendothelial migration is mediated by Notch1/MenaINV-initiated invadopodium formation. Sci Rep. 2016;6:37874.
36. Patsialou A, Wang Y, Pignatelli J, Chen X, Entenberg D, Oktay M, et al. Autocrine CSF1R signaling mediates switching between invasion and proliferation downstream of TGFbeta in claudin-low breast tumor cells. Oncogene. 2015;34(21):2721-31.
37. Sharma VP, Tang B, Wang Y, Duran CL, Karagiannis GS, Xue EA, et al. Live tumor imaging shows macrophage induction and TMEM-mediated enrichment of cancer stem cells during metastatic dissemination. Nat Commun. 2021;12(1):7300.
38. Wyckoff J, Gligorijevic B, Entenberg D, Segall J, Condeelis J. High-resolution multiphoton imaging of tumors in vivo. Cold Spring Harb Protoc. 2011;2011(10):1167-84.
39. Dovas A, Patsialou A, Harney AS, Condeelis J, Cox D. Imaging interactions between macrophages and tumour cells that are involved in metastasis in vivo and in vitro. J Microsc. 2013;251(3):261-9.
40. Bergers G, Hanahan D. Modes of resistance to anti-angiogenic therapy. Nat Rev Cancer. 2008;8(8):592-603.
41. Morgan C, Pollard JW, Stanley ER. Isolation and characterization of a cloned growth factor dependent macrophage cell line, BAC1.2F5. J Cell Physiol. 1987;130(3):420-7.
42. Schneider CA, Rasband WS, Eliceiri KW. NIH Image to ImageJ: 25 years of image analysis. Nat Methods. 2012;9(7):671-5.
43. Pignatelli J, Goswami S, Jones JG, Rohan TE, Pieri E, Chen X, et al. Invasive breast carcinoma cells from patients exhibit MenaINV- and macrophage-dependent transendothelial migration. Sci Signal. 2014;7(353):ra112.
44. Cabrera RM, Mao SPH, Surve CR, Condeelis JS, Segall JE. A novel neuregulin - jagged1 paracrine loop in breast cancer transendothelial migration. Breast Cancer Res. 2018;20(1):24.

Figure 1

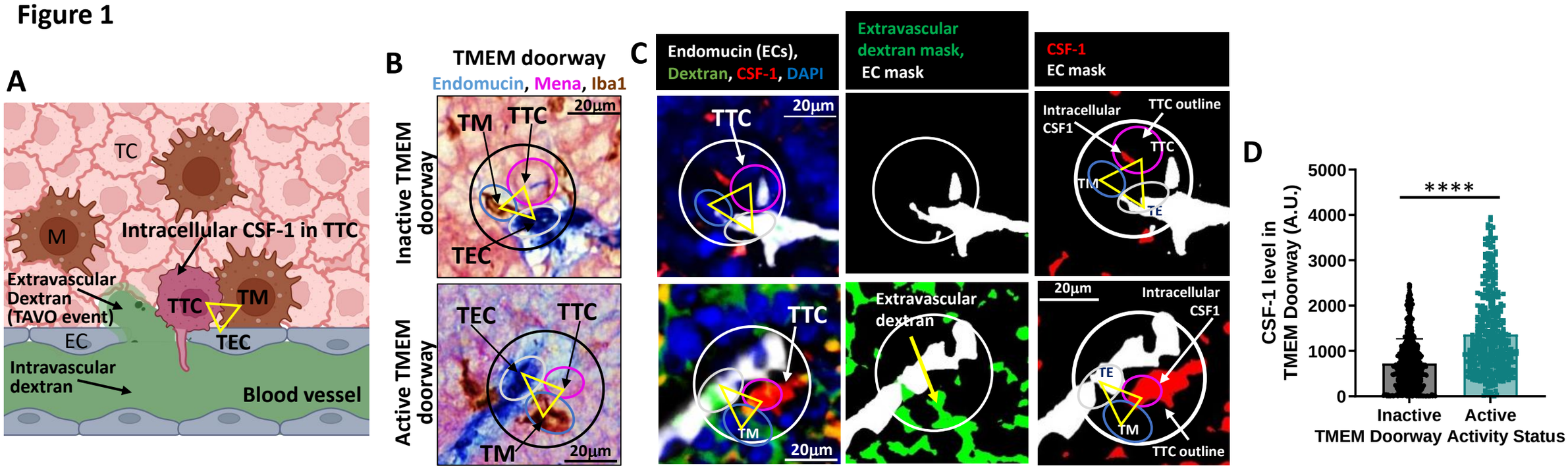
A
TC
M
Intracellular CSF-1 in TTC
Extravascular Dextran (TAVO event)
TTC
TM
TEC
EC
Intravascular dextran
Blood vessel
B
TMEM doorway
Endomucin, Mena, Iba1
Inactive TMEM doorway
Active TMEM doorway
TM
TTC
TEC
20µm
C
Endomucin (ECs), Dextran, CSF-1, DAPI
Extravascular dextran mask, EC mask
CSF-1 EC mask
Intracellular CSF1
TTC outline
Extravascular dextran
TE
D
CSF-1 level in TMEM Doorway (A.U.)
5000
4000
3000
2000
1000
0
****
Inactive
Active
TMEM Doorway Activity Status

Figure 2

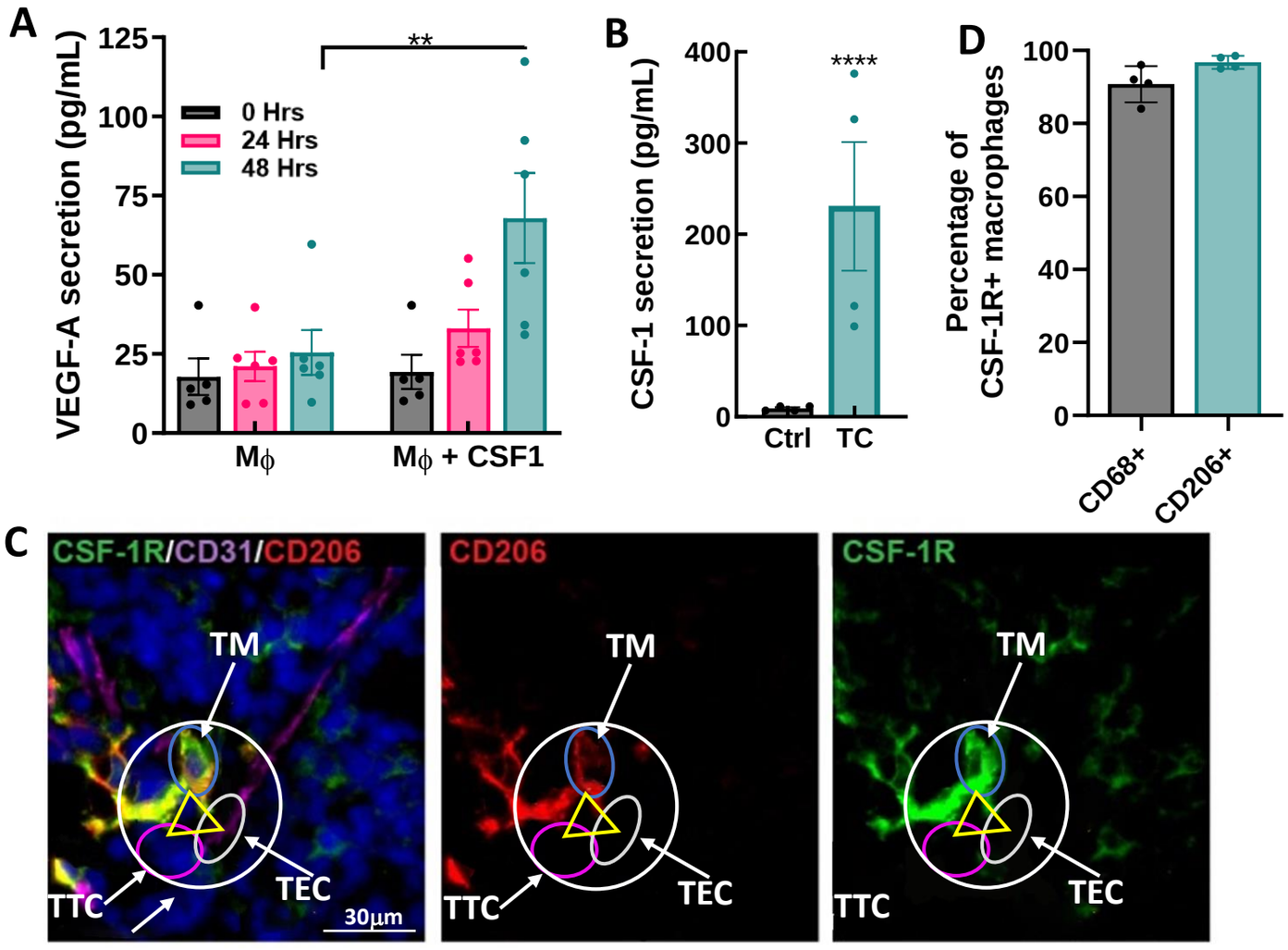
A
VEGF-A secretion (pg/mL)
125
100
75
50
25
0
**
0 Hrs
24 Hrs
48 Hrs
Mϕ
Mϕ + CSF1
B
CSF-1 secretion (pg/mL)
400
300
200
100
0
****
Ctrl
TC
D
Percentage of CSF-1R+ macrophages
100
80
60
40
20
0
CD68+
CD206+
C
CSF-1R/CD31/CD206
CD206
CSF-1R
TM
TTC
TEC
30µm

Figure 3

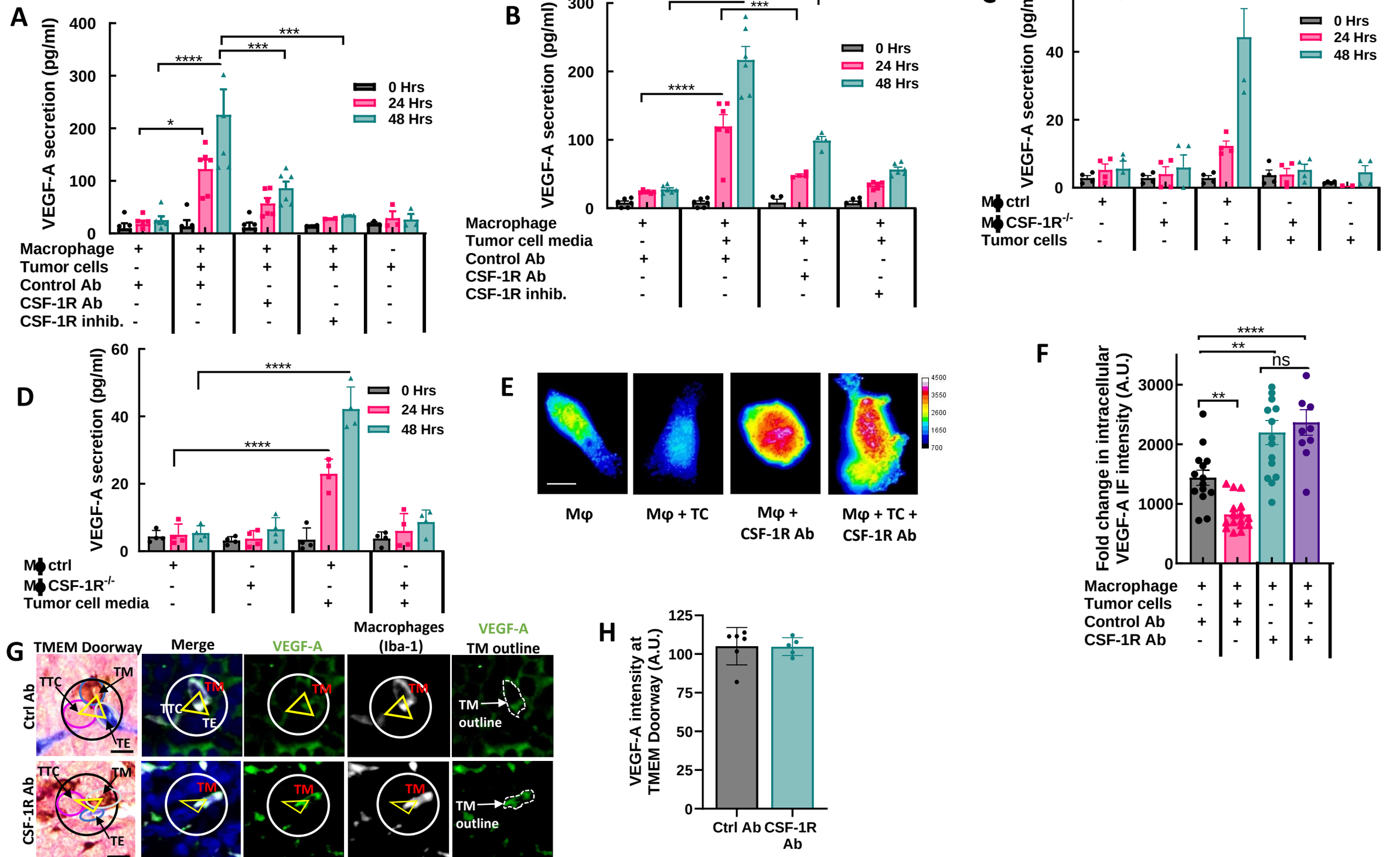
A
VEGF-A secretion (pg/ml)
0 Hrs
24 Hrs
48 Hrs
Macrophage
Tumor cells
Control Ab
CSF-1R Ab
CSF-1R inhib.
B
VEGF-A secretion (pg/ml)
Macrophage
Tumor cell media
Control Ab
CSF-1R Ab
CSF-1R inhib.
C
VEGF-A secretion (pg/ml)
Mφ ctrl
Mφ CSF-1R-/-
Tumor cells
D
VEGF-A secretion (pg/ml)
Mφ ctrl
Mφ CSF-1R-/-
Tumor cell media
E
Mφ
Mφ + TC
Mφ + CSF-1R Ab
Mφ + TC + CSF-1R Ab
F
Fold change in intracellular VEGF-A IF intensity (A.U.)
ns
Macrophage
Tumor cells
Control Ab
CSF-1R Ab
G
TMEM Doorway
Merge
VEGF-A
Macrophages (Iba-1)
VEGF-A
TM outline
Ctrl Ab
CSF-1R Ab
TTC
TM
TE
TM outline
H
VEGF-A intensity at TMEM Doorway (A.U.)
Ctrl Ab
CSF-1R Ab

Figure 4

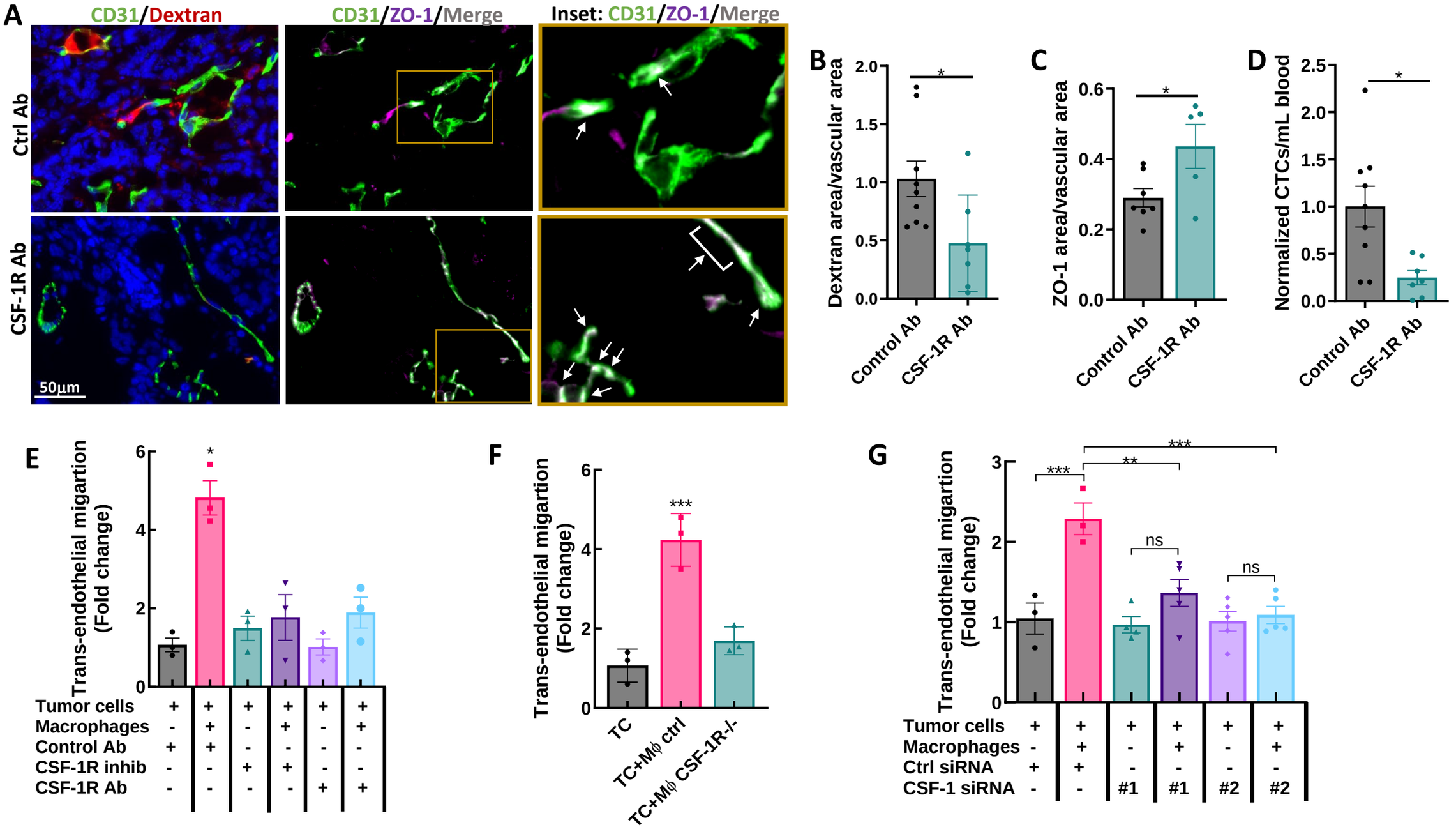
A
CD31/Dextran
CD31/ZO-1/Merge
Inset: CD31/ZO-1/Merge
Ctrl Ab
CSF-1R Ab
50µm
B
Dextran area/vascular area
Control Ab
CSF-1R Ab
C
ZO-1 area/vascular area
D
Normalized CTCs/mL blood
E
Trans-endothelial migartion (Fold change)
Tumor cells
Macrophages
Control Ab
CSF-1R inhib
CSF-1R Ab
F
TC
TC+Mϕ ctrl
TC+Mϕ CSF-1R-/-
G
Ctrl siRNA
CSF-1 siRNA
#1
#2
ns

Figure 5

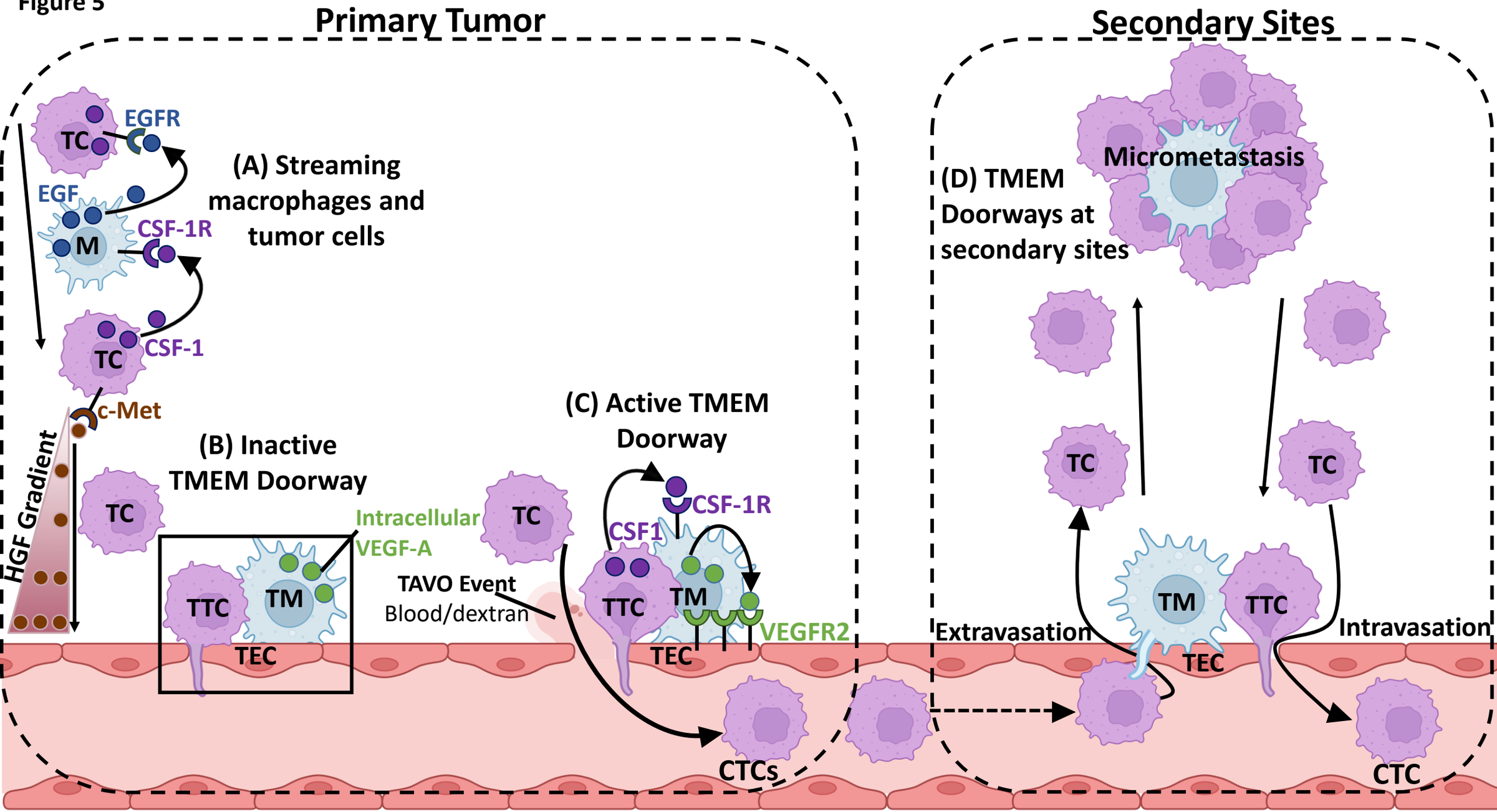
Primary Tumor
Secondary Sites
TC
EGFR
EGF
M
CSF-1R
(A) Streaming macrophages and tumor cells
TC
CSF-1
c-Met
HGF Gradient
(B) Inactive TMEM Doorway
TC
Intracellular VEGF-A
TTC
TM
TEC
TAVO Event
Blood/dextran
TC
(C) Active TMEM Doorway
CSF-1R
CSF1
TTC
TM
VEGFR2
TEC
CTCs
(D) TMEM Doorways at secondary sites
Micrometastasis
TC
TC
TM
TTC
Extravasation
Intravasation
TEC
CTC